Correlation of solar wind entropy and oxygen ion charge state ratio

A. C. Pagel and N. U. Crooker
Center for Space Physics, Boston University, Boston, Massachusetts, USA

T. H. Zurbuchen
Department of Atmospheric, Oceanic, and Space Science, University of Michigan, Ann Arbor, Michigan, USA

J. T. Gosling
Los Alamos National Laboratory, Los Alamos, New Mexico, USA

Received 28 April 2003; revised 4 September 2003; accepted 9 October 2003; published 29 January 2004.

[1] Both proton specific entropy and solar wind composition have been recognized in the past as markers of boundaries between what was originally slow and fast solar wind during the declining phase of the solar cycle, when the solar wind alternates between the two regimes. During the rising phase, when boundaries between regimes are not apparent, ACE SWICS and SWEPAM data from 1998–1999 show that O^{7+}/O^{6+} and proton specific entropy are well-correlated over the full range of complicated time variations. The correlation holds in spite of the fact that unlike O^{7+}/O^{6+}, entropy is not a constant of the solar wind flow. At solar maximum however, particularly in 2000, the correlation between entropy and O^{7+}/O^{6+} degrades. While the correlation inside known interplanetary coronal mass ejections (ICMEs) is much worse throughout 1998–2001, the correlation outside ICMEs also worsens at solar maximum, possibly owing to unidentified transient outflows. Outside ICMEs and shocks, entropy structures have decorrelation times of 5–40 hours and both $\ln(O^{7+}/O^{6+})$ and entropy have Gaussian distributions, consistent with their correlation. We conclude that except at solar maximum, the processes affecting entropy in nontransient solar wind act at time scales much smaller than the scales found here and that entropy is a good a proxy for O^{7+}/O^{6+}. *INDEX TERMS:* 2164 Interplanetary Physics: Solar wind plasma; 2169 Interplanetary Physics: Sources of the solar wind; 2111 Interplanetary Physics: Ejecta, driver gases, and magnetic clouds; 2102 Interplanetary Physics: Corotating streams; *KEYWORDS:* ion abundance ratios, proton entropy, solar maximum, solar wind source

Citation: Pagel, A. C., N. U. Crooker, T. H. Zurbuchen, and J. T. Gosling (2004), Correlation of solar wind entropy and oxygen ion charge state ratio, *J. Geophys. Res.*, *109*, A01113, doi:10.1029/2003JA010010.

1. Introduction

[2] Being able to clearly differentiate different types of solar wind is a first step in understanding its source. In the declining phase of the solar cycle through to solar minimum, the heliosphere has a relatively ordered structure; fast solar wind emanates from large, stable, polar coronal holes and slow solar wind flows from the magnetic equatorial region. While the precise origin of slow solar wind is not known, its boundaries have long been identified as stream interfaces. First observed as flow shears [*Siscoe et al.*, 1969], stream interfaces display distinct, often discontinuous, changes in proton density and temperature [*Burlaga*, 1974; *Gosling et al.*, 1978]. These combine to give a strong signature in proton specific entropy, which has also been used to identify stream interfaces [*Burlaga et al.*, 1990; *Siscoe and Intriligator*, 1993; *Burton et al.*, 1999].

[3] In Figure 1 we replot results from *Burlaga et al.* [1990] to emphasize the clarity of entropy as a marker for stream structure during the declining phase of the solar cycle. Figure 1 shows four solar rotations of data from 1974, with solar wind speed, proton specific entropy, proton temperature, and density plotted in the four panels. Marked on the plots are approximate stream interfaces as identified by *Burlaga et al.* [1990] (in red for the leading interface and in blue for the trailing interface). The leading interfaces (from slow to fast wind) are characterized by an abrupt decrease in density and a sharp increase in temperature. The trailing interfaces (from fast into slow wind) display the opposite characteristics, although the trailing edges tend to be less clearly defined than the leading edges. In Figure 1, they are predominately characterized by changes in the density. Between the streams (the regions between the blue and red lines) lies what *Burlaga et al.* [1990] term the heliospheric plasma sheet, with its distinctive high density and low temperature (see *Crooker* [2003] for a discussion of plasma sheet definitions).

[4] *Burlaga et al.* [1990] concluded that entropy is a good signature of stream structure in the inner heliosphere (as can be seen in Figure 1). Beyond 5 AU, however, the entropy signature becomes less clear, both because the streams start to coalesce and also because of the increase in entropy due

0148-0227/04/2003JA010010

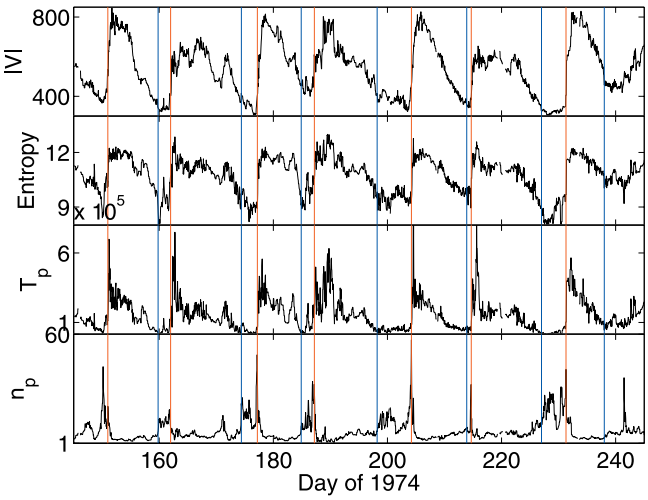

Figure 1. The 1974 Omniweb plasma data, replotted from *Burlaga et al.* [1990]. The top panel shows solar wind speed (km/s), the second panel shows proton specific entropy ($\ln(K/cm^{-3/2})$), the third shows proton temperature (K), and the bottom panel shows proton density (cm^{-3}). Stream interfaces are marked in red for the leading interface and in blue for the trailing interface.

to dynamic heating. That entropy increases with distance from the Sun (by a factor of 10% between 1 and 5 AU [*Burlaga et al.*, 1990]) is evidence that entropy is not a constant of solar wind flow.

[5] *Geiss et al.* [1995] reported distinct ion composition ratio populations in slow and fast wind. The O^{7+}/O^{6+} ratio is a function of freezing-in temperature in the corona. Unlike specific entropy, the ion ratio is fixed in the solar wind by five solar radii [*Ko et al.*, 1999; *von Steiger et al.*, 2000], becoming a constant of the solar wind flow. At that distance from the Sun, the solar wind is too diffuse for significant further interactions between solar wind ions and electrons that change the ionization states. Since this ratio is not modified by solar wind dynamic processes, it reflects conditions at the solar surface, with slow wind generally exhibiting higher O^{7+}/O^{6+} ratios than fast wind. Slow wind displays high O^{7+}/O^{6+} variability, perhaps indicative of the complex structure of its source regions on the solar surface [*Zurbuchen et al.*, 2000]. *Wimmer-Schweingruber et al.* [1997] showed that solar wind ion ratios (specifically for carbon and oxygen) exhibit sharp discontinuities at stream interfaces. They proposed that these boundaries were so clear as to provide an independent identification for these interfaces. On the other hand, *Zurbuchen et al.* [2002] reported that O^{7+}/O^{6+} exhibits a clear bimodal distribution during solar minimum, while at solar maximum the distribution is broad and unimodal, demonstrating a continuum of solar sources.

[6] *Burton et al.* [1999] showed that specific entropy tracked O^{7+}/O^{6+} in a negative sense in 1992–1993 Ulysses data during the declining phase of the solar cycle. In particular, they showed that entropy as well as O^{7+}/O^{6+} (and Mg/O) mark most stream interfaces on the trailing edges of fast flows. If, in general, entropy tracks O^{7+}/O^{6+} well, it has the advantage of high temporal resolution. For instance, *Wimmer-Schweingruber et al.* [1997] used density and temperature data to pin down the precise times of the stream interfaces for O^{7+}/O^{6+} signatures.

[7] In this paper, we test for the first time whether specific entropy tracks O^{7+}/O^{6+} during the rising phase of the solar cycle and into solar maximum, when corotating streams are less prevalent, while interplanetary coronal mass ejections (ICMEs) and shocks are more frequent. Our focus shifts from the stream interfaces analyzed in previous studies to variations in entropy and O^{7+}/O^{6+} as a function of time. We will show that these two parameters not only reflect high-speed and low-speed regimes but that they also track each other through solar wind flows with no clear boundaries on the rising phase of the solar cycle. We also show that the correlations break down at solar maximum and during ICMEs. We note that by restricting our analysis to O^{7+}/O^{6+}, we are not addressing differences between different ion ratios and ion abundances [c.f. *McComas et al.*, 2002].

2. Analysis

[8] We use 1-hour averaged data from the SWICS and SWEPAM instruments on the ACE spacecraft from 1998 to 2001. Details of the ACE mission as a whole can be found in the work of *Stone et al.* [1998], while details for SWICS and SWEPAM experiments can be found in the work of *Gloeckler et al.* [1998] and *McComas et al.* [1998], respectively. Proton specific entropy is proportional to $ln(T_p/n_p^{\gamma-1})$, where T_p and n_p represent the proton temperature and number density, respectively. In this paper we use $\gamma = 1.5$, consistent with values measured in the solar wind [*Siscoe and Intriligator*, 1993; *Burton et al.*, 1999]. While in the absence of shocks and other dissipative processes, specific proton entropy (hereafter just called entropy) would be a constant of the flow [*Siscoe and Intriligator*, 1993], we are not claiming that it is a true representation of entropy in the solar wind. Our use is consistent with prior work by *Burlaga et al.* [1990], *Siscoe and Intriligator* [1993], and *Burton et al.* [1999].

2.1. Correlation

[9] Before analyzing the correlation of entropy and O^{7+}/O^{6+}, we use a short interval of data from 1998 to illustrate

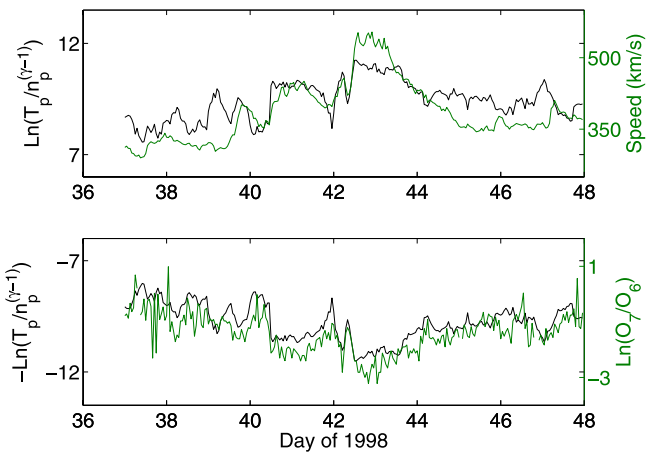

Figure 2. Plots of entropy ($\ln(K/cm^{-3/2})$), solar wind speed (km/s), and $\ln(O^{7+}/O^{6+})$ for 12 days of 1998 data.

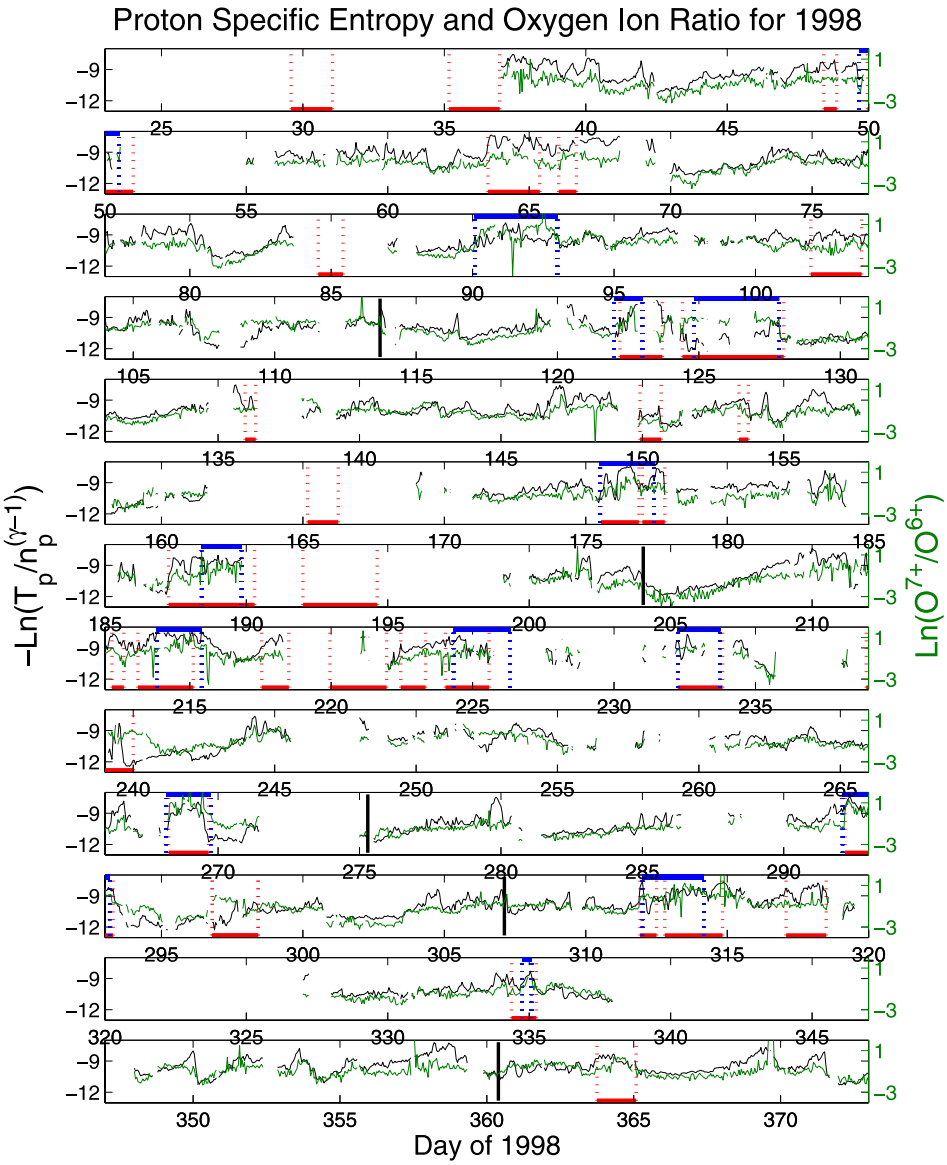

Figure 3. Specific proton entropy (ln(K/cm$^{-3/2}$)) and oxygen ion ratio of O^{7+}/O^{6+} for 1998 using ACE SWEPAM and SWICS data, plotted per Carrington rotation. We plot negative proton entropy to emphasize the correlation. Both are plotted on a log scale (with entropy in black), and ICME events are indicated in red and high iron charge distribution events in blue. Shocks from the ACE shock list, not obviously related to ICME events, have been marked using thick vertical black lines.

how closely these parameters can track each other. The correlation of entropy with speed seen in Figure 1, continued on the approach to solar maximum, as shown in the top panel of Figure 2. On the other hand, the solar wind has considerably more structure than is evident from looking at the solar wind speed alone [*Bame et al.*, 1977; *Feldman et al.*, 1977; *Zurbuchen et al.*, 2000]. *Zurbuchen et al.* [2000] show that O^{7+}/O^{6+} is a sensitive indicator of solar wind variability. During the declining phase of the solar cycle, O^{7+}/O^{6+} has a bimodal distribution, expressing the clear differences between fast and slow wind. At solar maximum, however, there exists a continuum of O^{7+}/O^{6+} ratios characterizing the complexity of solar wind source regions and production mechanisms. Figure 2 shows that entropy also displays greater variability in slow wind than the wind speed itself, correlating well with the O^{7+}/O^{6+} signatures in the second panel. Since O^{7+}/O^{6+} is thought to be a robust indicator of solar wind source region, such a correlation suggests that entropy too, at least at times, can be used as a sensitive source region tracer.

[10] Looking now at longer periods, Figures 3 to 6 show plots of O^{7+}/O^{6+} ratios from SWICS and entropy from SWEPAM for 1998 to 2001. The plots are stacked according to Carrington rotation, and the ion ratio is plotted on a natural log scale for better comparison with the entropy. ICME times, bordered in red, come from a comprehensive list compiled by *Cane and Richardson* [2003]. Similarly, high iron charge distribution events, considered a signature

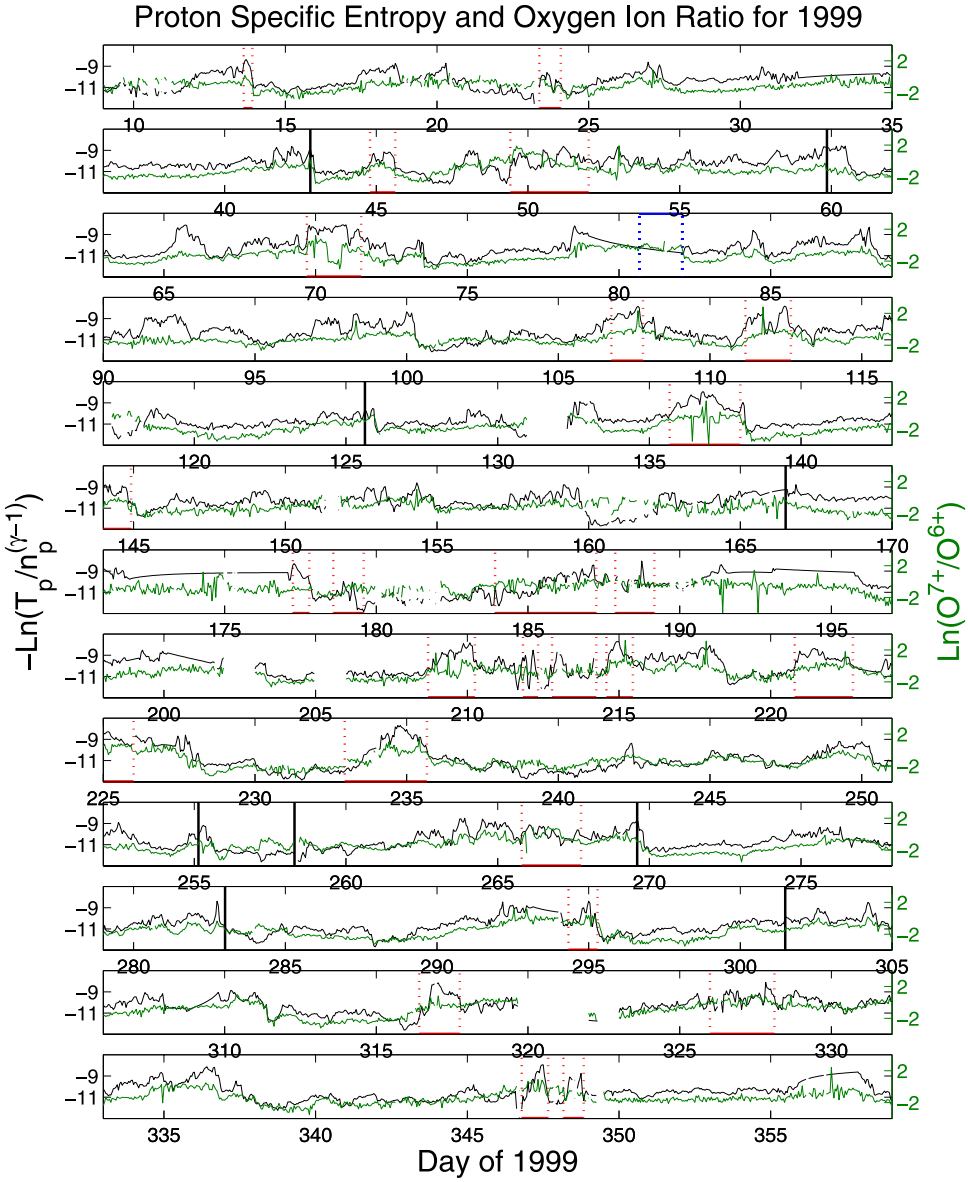

Figure 4. As for Figure 3 except for 1999.

of ICMEs, are bordered in blue and come from a list compiled by *Lepri et al.* [2001] from ACE data for 1998 to mid-2000. All are plotted for 1998, but for 1999–2000 only those events not associated with ICMEs are plotted to avoid clutter. Shocks from the ACE website (courtesy of C.W. Smith and R.M. Skoug), which are not immediately followed by, or found within, an ICME are marked with a thick black vertical line.

[11] The correlation between entropy and $\ln(O^{7+}/O^{6+})$ is immediately evident in Figures 3 and 4, particularly for days 37–48, 70–84, and 200–211 in 1998 and days 270–283, 306–315, and 329–345 in 1999. Also evident is the lack of correlation throughout most of 2000 (Figure 5), while the correlation recovers somewhat in 2001 (Figure 6). It is also clear that the number of shocks and ICMEs increases significantly for 2000 and 2001 at solar maximum, where long stretches of "stable" solar wind were rare. The occasional straight lines evident in the entropy for years 1999–2000 are where SWEPAM data have been linearly interpolated. We do not use these periods in our study.

[12] To check that the apparent correlation is not just an artifact of the scales we use for our figures, we normalized both parameters for the 1998 data by subtracting their total mean and dividing by their total standard deviation. We then proceeded in the same way as for Figure 3. The small sample shown in Figure 7 demonstrates that the correlation is unaffected for that interval. Similarly, we have checked that an entropy calculation including both protons and helium ions (using a formula given by J. Gloag, private communication, 2003) does not affect the correlations we observe. We present unnormalized results using only proton specific entropy in this paper for easier interpretation.

2.2. Time Scales

[13] Following *Zurbuchen et al.* [2000], we perform a timescale analysis of entropy variations. *Zurbuchen et al.*

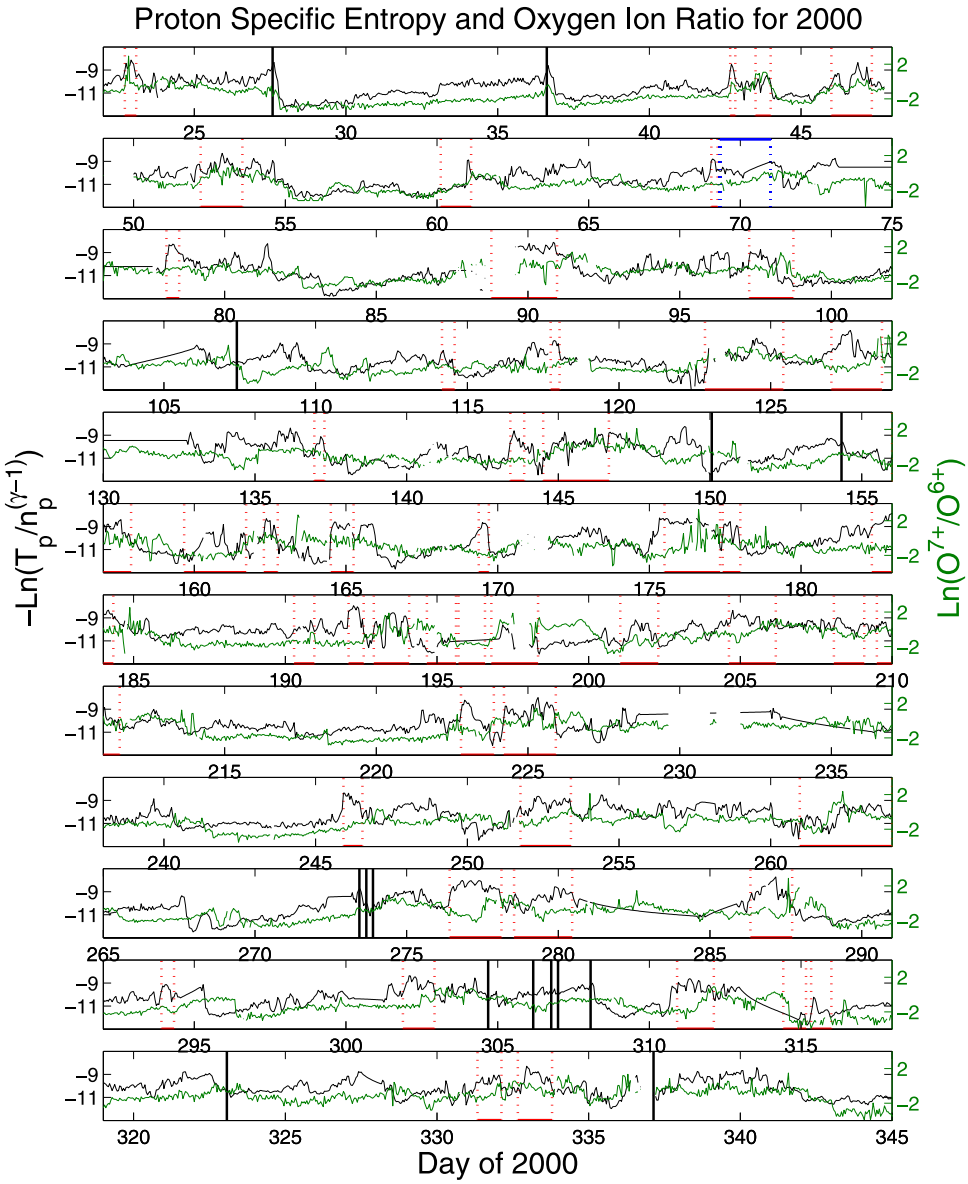

Figure 5. As for Figure 3 except for 2000.

[2000] analyzed O^{7+}/O^{6+} signatures in ACE SWICS data for days 140–148 in 1998, where the days were chosen to lie within a single sector of magnetic polarity and away from ICME signatures. They concluded that the sharp variations in O^{7+}/O^{6+} signatures were indicators of "finite solar wind sources emitting wind of a particular composition." *Zurbuchen et al.* [2000] reported a 1/e decorrelation time of about 10 hours within their chosen 8-day period for the typical coherent size of a particular compositional structure. They relate this time to the size of coronal loops at the Sun under the assumption that the O^{7+}/O^{6+} structures are released from the loops through interchange reconnection with open field lines [*Fisk et al.*, 1999]. Here, for each year, we identify periods of at least 6 days which lie outside both ICME events and the high iron charge distribution events and do not contain shocks on the ACE shock list. We then calculate the entropy autocorrelation for lags up to 50 hours. On a semilog plot of the autocorrelation against time lag, a straight line indicates an exponential decay. The decorrelation time, $\tau_{1/e}$, is taken to be that time where the autocorrelation falls to 1/e. Three examples from 1998 are shown in Figure 8, with the dashed lines marking $\tau_{1/e}$. Tables 1 to 4 give the decorrelation times for all the time periods greater than 6 days for 1998–2001.

[14] The decorrelation times range between 4 and 41 hours, which correspond to radial distances of about 0.05–0.4 AU. For days 140–148, the time period analyzed by *Zurbuchen et al.* [2000] (see middle panel of Figure 8), we get a decorrelation time of 9 hours for entropy, consistent with their 10-hour timescale for O^{7+}/O^{6+}. With our entire data set, we find timescales up to four times larger. There is no dependence of these characteristic times on the interval length, and the range of timescales on the rising phase (1998 and 1999) are approximately the same as at solar maximum (2000 and 2001). The wide and reasonably continuous range is consistent with a continuous range of

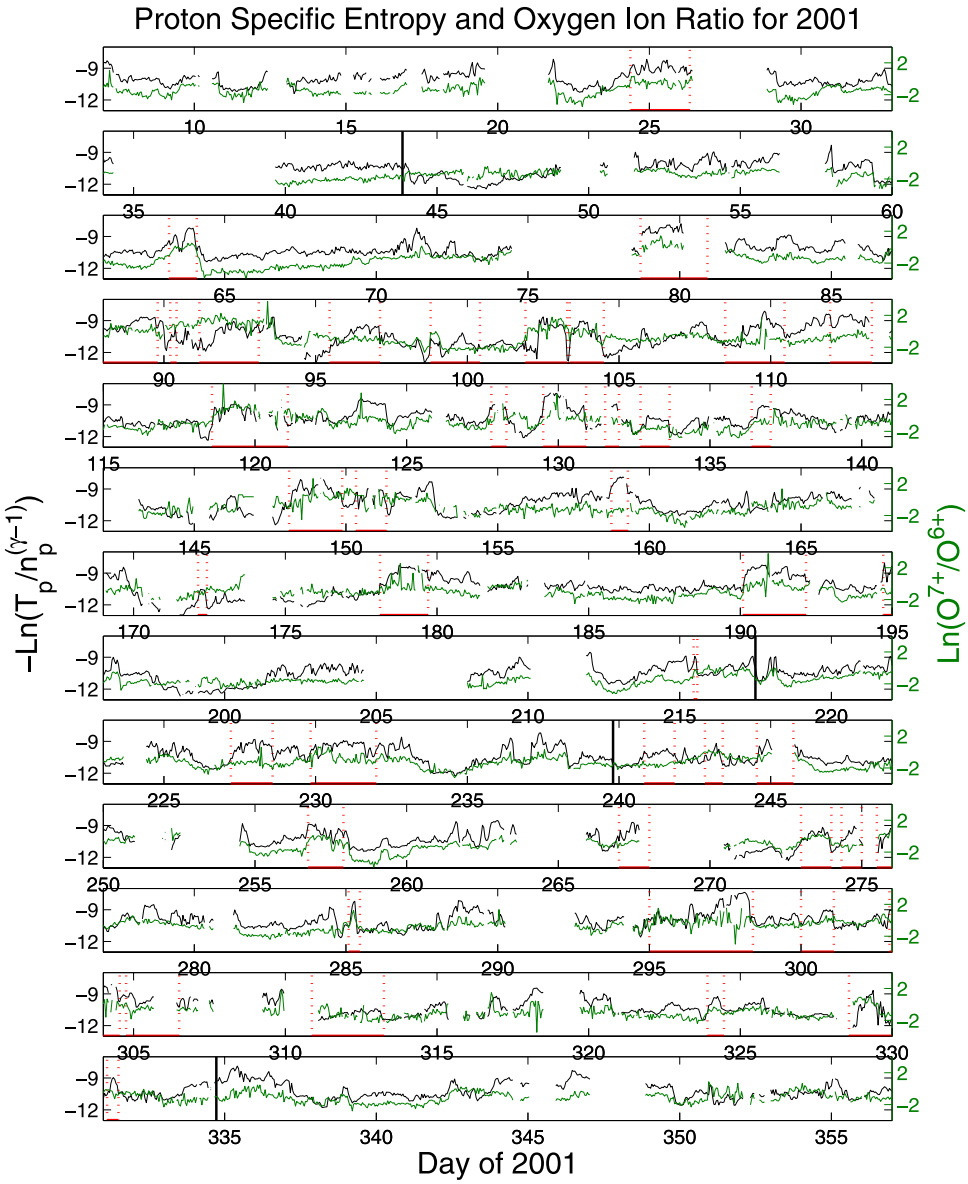

Figure 6. As for Figure 3 except for 2001.

coronal loop sizes and reconnection processes as a source of slow wind.

[15] Since the time periods selected for the autocorrelation analysis represent reasonably long continuous data periods, lacking obvious large scale transient disturbances, we have also calculated the correlation coefficients, ρ, between the (negative) proton specific entropy and the natural log of oxygen ion ratio for these periods. We note that correlation coefficients depend on the variability of the parameters and thus the values obtained should be treated more qualitatively than quantitatively.

[16] The correlation coefficients are given in the right-hand column of Tables 1 to 4, along with the mean for each year. The correlations for both 1998 and 1999 are reasonably high. The selected intervals in 1998 all have correlations higher than 0.6 and, while 1999 has several intervals with poor correlation, it also has a large number of highly correlated intervals. In 2000, the correlations drop off

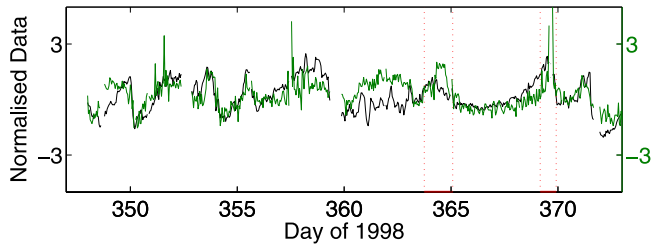

Figure 7. Normalized specific proton entropy (ln(K/cm$^{-3/2}$)) and oxygen ion ratio of O^{7+}/O^{6+} for Carrington rotation 1994. Both are plotted on a log scale (with entropy in black). The two ICME events in this period are marked in red. This Carrington rotation extends from 1998 into the beginning of 1999 (days greater than 365).

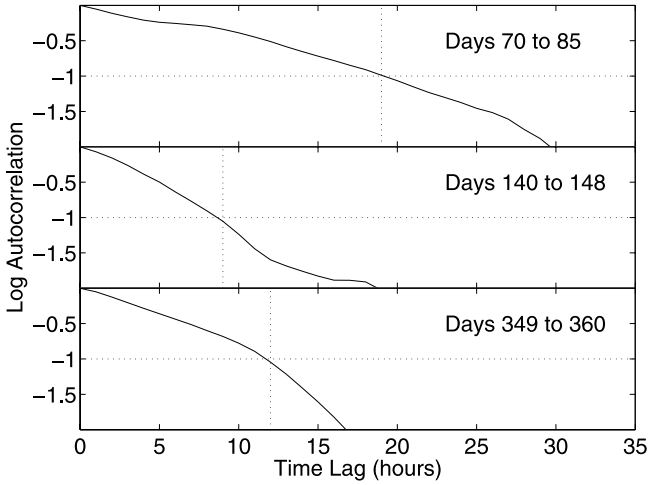

Figure 8. Entropy autocorrelation plots indicating scale sizes of entropy structures in the slow solar wind for these intervals. The dashed vertical lines mark the decorrelation time, $\tau_{1/e}$. The middle plot coincides with the data used by *Zurbuchen et al.* [2000].

dramatically, with only three out of ten intervals showing values >0.6, while 2001 shows an increase in the correlation, with five out seven intervals having values $\geq$0.55. We note that in 2000 and 2001 the nontransient intervals of solar wind are much rarer than on the rising phase of the solar cycle, so we have shorter intervals for correlation analysis.

2.3. Probability Distributions of $\ln(O^{7+}/O^{6+})$ and Entropy

[17] In section 2.2 we showed that in periods of relatively stable solar wind, where large-scale transient disturbances are absent, entropy and $\ln(O^{7+}/O^{6+})$ are well correlated on the rise to solar maximum. Here we consider the probability distributions of these quantities. *Zurbuchen et al.* [2000] calculated the probability distribution of O^{7+}/O^{6+} for their 8-day period and concluded that it was lognormal, i.e., $\ln(O^{7+}/O^{6+})$ exhibited a normal distribution, with mean -1.32 and standard deviation 0.45. We use our full 4 years of data to calculate the probability distributions of entropy and $\ln(O^{7+}/O^{6+})$. If both the oxygen ion ratio and the entropy reflect a similar variability on the solar surface, then they should follow the same distribution. Being similarly distributed is consistent with their correlation, if not in itself a sufficient condition for the parameters to be correlated.

[18] To calculate the probability distributions, we used all hourly values of the oxygen ion ratios and entropy from the periods of solar wind given in Tables 1 to 4. We normalized each data set by subtracting the mean, μ_i, and dividing by the standard deviation, σ_i, to obtain parameters $P_i = (X_i - \mu_i)/\sigma_i$, where X_i is either $\ln(O^{7+}/O^{6+})$ or $\ln(T/n^{\gamma-1})$. After binning both parameters into histograms, we found their probability distribution by dividing the count for each bin by the total count for all the bins and the width of that particular bin. The resultant probability distributions appear on the same plot in the top panel of Figure 9, where the standard normal distribution is shown as a continuous red line. Also shown are the mean and standard deviation of each parameter before normalization.

[19] The fit to the standard normal distribution in the top panel of Figure 9 is excellent, and the mean of $\ln(O^{7+}/O^{6+})$ (-1.49) is close to that found by *Zurbuchen et al.* [2000] (-1.32), while the standard deviation (0.76) is greater than their standard deviation (0.45). This is expected given the much larger data set we are using here. The standard deviation of the natural log of the oxygen ion ratio and the entropy are of a similar order of magnitude, suggesting that they have similar levels of variability. To check further the quality of the fit to the tails of the distribution, we plot the same data on a semilog scale in the bottom panel of Figure 9. It is evident that the fits remain excellent for both parameters, so we can be confident in asserting that both

Table 1. The 1/e Correlation Times (Column 2) for Various Time Periods in 1998, Selected for Reasonable Length and Lack of ICME and Shock Events[a]

Year	Days	$\tau_{1/e}$ hours	ρ -entropy, O^{7+}/O^{6+}
1998	37–48	19	0.78
1998	70–85	19	0.78
1998	114–120	7	0.70
1998	140–148	9	0.63
1998	205–211	30	0.87
1998	276–285	14	0.61
1998	300–307	20	0.84
1998	349–360	12	0.60
Mean		16.3	0.73

[a]Also listed are the correlation coefficients, ρ, between negative proton entropy and O^{7+}/O^{6+} (column 3).

Table 2. Same as Table 1 for 1999

Year	Days	$\tau_{1/e}$ hours	ρ -entropy, O^{7+}/O^{6+}
1999	15–22	16	0.34
1999	25–31	9	0.70
1999	36–42	5	0.69
1999	53–59	5	0.18
1999	61–68	11	0.72
1999	72–79	9	0.84
1999	83–106	16	0.62
1999	115–125	11	0.38
1999	146–166	15	−0.05
1999	237–255	25	0.56
1999	259–265	26	0.79
1999	270–283	26	0.77
1999	284–294	36	0.80
1999	306–315	22	0.81
1999	329–345	41	0.81
1999	350–358	27	0.74
Mean		18.3	0.61

Table 3. Same as Table 1 for 2000

Year	Days	$\tau_{1/e}$ hours	ρ -entropy, O^{7+}/O^{6+}
2000	28–36	41	0.81
2000	62–68	10	−0.05
2000	80–87	26	0.66
2000	108–113	17	−0.25
2000	213–221	8	0.17
2000	236–245	14	0.25
2000	265–273	22	0.01
2000	295–301	9	0.02
2000	324–330	12	−0.14
2000	338–345	36	0.71
Mean		18.9	0.22

Table 4. Same as Table 1 for 2001

Year	Days	$\tau_{1/e}$ hours	ρ -entropy, O^{7+}/O^{6+}
2001	65–73	6	0.55
2001	121–126	9	0.24
2001	160–167	22	0.66
2001	183–189	4	0.39
2001	218–222	3	0.74
2001	233–239	9	0.84
2001	335–344	21	0.60
Mean		10.6	0.57

$\ln(O^{7+}/O^{6+})$ and $\ln(T/n\gamma^{-1})$ follow normal distributions. That is O^{7+}/O^{6+} and $T/n^{\gamma-1}$ are both lognormal.

[20] The fact that $\ln(O^{7+}/O^{6+})$ and $\ln(T/n^{\gamma-1})$ remain well correlated outside ICMEs and shocks implies that the processes heating the solar wind and increasing its entropy, must be acting at much smaller scales than the typical timescales found in section 2.2. If they were acting at larger-scale sizes, the entropy distribution would be likely to have a different shape than the $\ln(O^{7+}/O^{6+})$ distribution, which is thought to be preserved from the Sun. Increases of entropy at smaller scales however, as long as they are relatively uniform, act only to change the mean of the distribution.

3. Interplanetary Coronal Mass Ejections

[21] Under time-varying conditions and heat-generating processes, entropy is not a constant of solar wind flow. Shocks are known to modify the entropy, reducing its correlation with $\ln(O^{7+}/O^{6+})$, and it might be expected that ICMEs do, as well. Figures 3 to 6 seem inconclusive on this point; there are some ICME events where the correlation between entropy and $\ln(O^{7+}/O^{6+})$ obviously breaks down, e.g., for days 296–298 or days 311–315 in 1998 but other events where the correlation seems to remain high, e.g., days 175–178 or days 150–154 in 1998. Calculating correlation coefficients over short timescales, certainly over timescales of less than a day, encompassing less than 25 data points, can be misleading, so we have not calculated correlation coefficients for all the ICME events for which we have data. However, we have calculated coefficients for all ICME events lasting at least one and a half days, combining two or more ICME events if they occurred within a day of each other, and these are listed in Tables 5 to 8. These correlation coefficients will naturally be less reliable than those calculated above for the non-ICME intervals, all of which were of at least 6 days duration. Nonetheless, the poor correlation in these long-lasting ICME events is noticeable for all years, with several events even exhibiting negative correlation. Since the O^{7+}/O^{6+} ratios are frozen into the solar wind within a few solar radii of the Sun, from the reduced correlations we infer that it is the entropy that is being affected by some dynamic processes associated with the ICME.

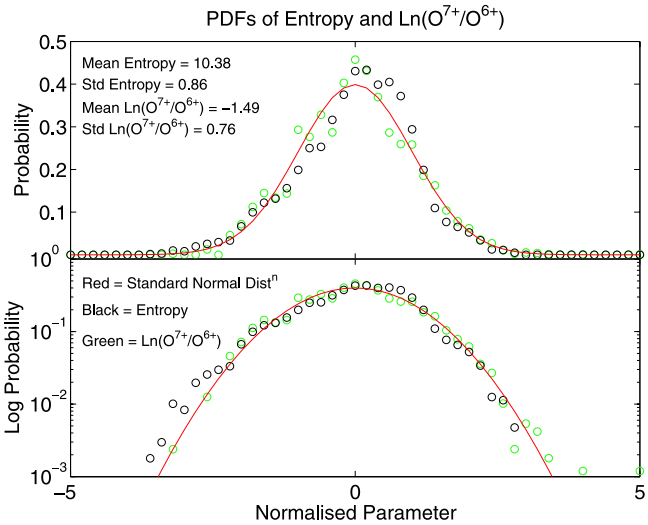

Figure 9. The distributions of $\ln(T/n^{\gamma-1})$ and $\ln(O^{7+}/O^{6+})$, where both parameters have been normalized. Their mean and standard deviation are given in the top panel. Entropy is plotted in black and oxygen in green. The red line is the standard normal distribution (i.e., the normal distribution with mean zero and standard deviation one). Both parameters seem to fit this distribution well. To check for fits at the tails of the distribution, we also plot the same thing on semilog scale (bottom panel) and we see that the fit remains excellent.

Table 5. Correlation Coefficients Between ln (O^{7+}/O^{6+}) and Negative Proton Entropy for ICME Events in 1998

Year	ICME Days	ρ -entropy(p), O^{7+}/O^{6+}
1998	63.5–66.7	0.28
1998	102.0–103.8	−0.01
1998	122.2–128.0	−0.27
1998	175.5–177.8	0.27
1998	187.3–190.3	0.36
1998	212.3–215.1	0.31
1998	220.0–223.3	0.76
1998	224.0–225.6	−0.07
1998	232.3–233.8	−0.29
1998	296.8–298.4	−0.63
1998	311.9–314.8	0.25
Mean		0.08

[22] To check for any systematic patterns in the correlations that depend on whether the ICME was a magnetic cloud or not, we use the identifications of *Cane and Richardson* [2003] based on criteria originally set out by *Burlaga et al.* [1981]. Neither the actual value of the correlations, nor the relative values of the entropy and oxygen ion ratios, depended on whether the ICME was a magnetic cloud or not.

Table 6. Same as Table 5 for 1999

Year	ICME Days	ρ -entropy(p), O^{7+}/O^{6+}
1999	49.4–52.0	−0.38
1999	69.7–71.5	−0.02
1999	135.7–138.0	−0.15
1999	177.3–179.6	0.23
1999	183.9–189.2	−0.03
1999	208.7–210.3	0.20
1999	211.8–214.3	0.12
1999	220.8–222.7	−0.07
1999	233.0–235.7	0.71
1999	265.8–267.8	0.09
1999	326.0–328.1	0.08
1999	346.8–348.8	0.26
Mean		0.09

Table 7. Same as Table 5 for 2000

Year	ICME Days	ρ -entropy(p), O^{7+}/O^{6+}
2000	88.8–91.0	0.05
2000	122.8–125.4	0.20
2000	127.0–128.7	−0.52
2000	143.4–146.7	0.21
2000	156.0–157.9	0.18
2000	159.7–162.8	0.32
2000	175.5–178.0	−0.29
2000	182.3–184.3	−0.06
2000	192.1–194.1	−0.27
2000	204.6–206.2	−0.60
2000	208.1–211.5	0.31
2000	222.8–225.9	0.10
2000	251.8–253.4	0.37
2000	261.0–264.0	0.35
2000	276.4–280.5	−0.52
2000	331.3–333.8	−0.02
Mean		0.01

[23] We also looked for any dependence of the correlation within ICMEs on mean entropy and oxygen ion ratios but found none. Figures 10 and 11 show the correlation plotted against entropy and ln(O^{7+}/O^{6+}), respectively, both for times without ICMEs or shocks from Tables 1 to 4 and ICME times from Tables 5 to 8. Both figures show clearly that the correlation outside ICMEs is generally much higher than that within and that no obvious patterns emerge. The range of values for both parameters is greater within ICMEs than within the non-transient solar wind, with values of the oxygen ion ratio being generally higher (Figure 11) and the entropy generally lower (Figure 10), due primarily to the lower temperatures inside ICMEs.

[24] We note that all but three of the high iron charge distribution events given by *Lepri et al.* [2001] coincide with the ICMEs identified by *Cane and Richardson* [2003]. In 1999 and 2000, two of these events overlap with a period lacking SWEPAM data, but the third event on days 90–94 in 1998 seems to coincide with a period of poor correlation for entropy and oxygen ion ratio. Detailed data for this period suggest that the lack of correlation is probably due to some anomalous ionisation at the Sun leading to variable, but high, oxygen and iron composition signatures.

Table 8. Same as Table 5 for 2001

Year	ICME Days	ρ -entropy(p), O^{7+}/O^{6+}
2001	24.4–26.3	0.03
2001	78.7–80.9	0.04
2001	87.3–90.4	−0.12
2001	91.2–93.1	−0.07
2001	95.5–97.1	0.25
2001	98.8–100.4	0.18
2001	101.9–104.5	0.25
2001	108.5–110.5	0.15
2001	118.6–121.1	0.46
2001	129.5–132.0	0.43
2001	148.1–151.3	−0.24
2001	178.1–179.7	0.26
2001	190.1–192.2	0.07
2001	229.8–232.0	−0.05
2001	273.0–275.0	0.27
2001	295.0–298.4	−0.11
2001	302.9–306.5	0.52
2001	310.9–313.3	−0.61
2001	328.6–331.5	0.36
Mean		0.11

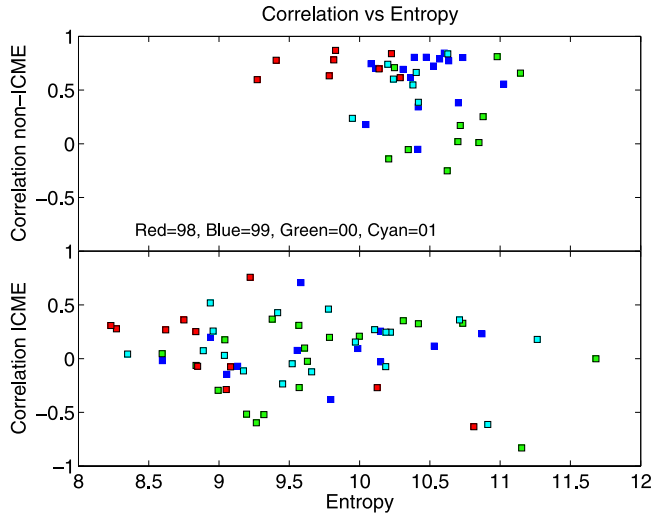

Figure 10. Correlation between proton specific entropy and ln(O^{7+}/O^{6+}) plotted against mean entropy. The top panel is for time periods outside ICME, high-iron or shock events from Tables 1 to 4, and the bottom panel is for ICME events given in *Cane and Richardson* [2003] and Tables 5 to 8. Events are color-coded so that red signifies 1998, blue signifies 1999, green signifies 2000, and cyan signifies 2001.

4. Discussion and Conclusions

[25] We have used ACE SWICS and SWEPAM data from 1998 through to 2001 to investigate correlations between O^{7+}/O^{6+} and proton specific entropy in the solar wind at 1 AU. We have shown that on the rise to solar maximum, 1998–1999, entropy is in remarkably good correlation with O^{7+}/O^{6+}, in spite of the high variability of both parameters

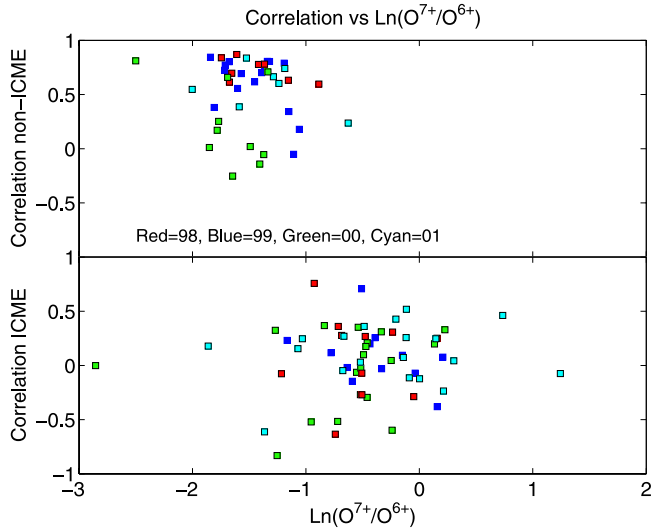

Figure 11. As for Figure 10 except the correlations are plotted against ln(O^{7+}/O^{6+}) instead. Note the wider range of O^{7+}/O^{6+} in ICMEs than outside them.

in this time period. We calculated correlation coefficients for periods greater than 6 days that did not include large-scale transient disturbances or shocks and found reasonably high values for the 2 years, often higher than 0.75. At solar maximum in 2000 however, the correlation between the two parameters drops sharply, with some recovery evident in 2001.

[26] The results imply that outside ICMEs during the rising phase of the solar cycle, the proton specific entropy is a good indicator of solar wind stream structure over the continuum of dynamic states found by *Zurbuchen et al.* [2002]. Thus except at the peak of solar maximum, entropy provides a reasonably good tracer for stream sources in cases where O^{7+}/O^{6+} data are lacking and in cases where high temporal resolution is required. Since entropy is not a constant of the flow, its continuing correlation with O^{7+}/O^{6+} implies that the variability we see in entropy at 5–40 hour timescales, rather than entropy itself, is preserved from its solar source. We suggest that the processes which increase the entropy in the solar wind must be acting at scales much smaller than 5–40 hours, and they must be acting consistently. These conclusions are substantially supported by the fact that entropy and $\ln(O^{7+}/O^{6+})$ have the same probability distribution.

[27] Candidate processes for increasing entropy are those which directly result in proton heating, since protons are hotter than they should be if the solar wind were expanding adiabatically. One possibility is turbulent heating. The solar wind is known to be highly turbulent in both slow and fast wind [e.g., *Roberts and Goldstein*, 1991; *Goldstein and Roberts*, 1995], and the turbulent cascade transfers heat through the successively smaller scales until finally dissipating at the proton gyroscale. Thus turbulence heats protons on timescales of about 4 s in the solar wind. For more on these issues see, e.g., *Coleman* [1968] or *Li et al.* [2001]. An investigation of this hypothesis should prove an interesting future study.

[28] Using lists of ICMEs provided by *Cane and Richardson* [2003], we found that the correlation between entropy and O^{7+}/O^{6+} was markedly poorer in ICME events compared to non-transient events. Since most ICMEs have depressed proton temperature [*Gosling et al.*, 1973; *Richardson and Cane*, 1995], it is difficult to assess whether the poor correlations are the result of interplanetary dynamics or are due to solar processes during CME formation. One likely candidate for heating that spans the two regimes is large-scale reconnection in the wake of CME liftoff, as evidenced in X ray arcade events [e.g., *Gosling et al.*, 1995]. Reconnection in the wake of CMEs lasts for at least a day and probably longer [e.g., *Crooker et al.*, 2002]. Whatever causes the breakdown of correlation in ICMEs may also be responsible for the poor correlations found outside ICMES in 2000, at solar maximum. This would be the case if much of the solar wind at that time contained transient material not recognised as ICMEs [e.g., *Crooker et al.*, 2002].

[29] **Acknowledgments.** C. Pagel and N. Crooker are supported by the National Science Foundation under grant number ATM-0119700. Work by J. Gosling has been performed under the auspices of the U.S. Department of Energy with support from NASA under the ACE program.

[30] Shadia Rifai Habbal thanks David J. McComas and another referee for their assistance in evaluating this paper.

References

Bame, S. J., J. R. Asbridge, W. C. Feldman, and J. T. Gosling (1977), Evidence for a structure-free state at high solar wind speeds, *J. Geophys. Res.*, *82*, 1487–1492.

Burlaga, L. F. (1974), Interplanetary stream interfaces, *J. Geophys. Res.*, *79*, 3717–3725.

Burlaga, L. F., E. Sittler, F. Mariani, and R. Schwenn (1981), Magnetic loop behind an interplanetary shock: Voyager, Helios and IMP 8 observations, *J. Geophys. Res.*, *86*, 6673.

Burlaga, L. F., W. H. Mish, and Y. C. Whang (1990), Coalescence of recurrent streams of different sizes and amplitudes, *J. Geophys. Res.*, *95*, 4247–4255.

Burton, M. E., M. Neugebauer, N. U. Crooker, R. von Steiger, and E. J. Smith (1999), Identification of trailing edge solar wind stream interfaces: A comparison of Ulysses plasma and composition measurements, *J. Geophys. Res.*, *104*, 9925–9932.

Cane, H. V., and I. G. Richardson (2003), Interplanetary coronal mass ejections in the near-Earth solar wind during 1996–2002, *J. Geophys. Res.*, *108*(A4), 1156, doi:10.1029/2002JA009817.

Coleman, P. J. (1968), Turbulence, viscosity and dissipation in the solar wind plasma, *Astrophys. J.*, *153*, 371–388.

Crooker, N. U. (2003), Heliospheric current and plasma sheet structure, in *Solar Wind Ten*, edited by M. Velli et al., *AIP Conf. Proc.*, *679*, 93–97.

Crooker, N. U., J. T. Gosling, and S. W. Kahler (2002), Reducing heliospheric magnetic flux from CMEs without disconnection, *J. Geophys. Res.*, *107*(A2), 1028, doi:10.1029/2001JA000236.

Feldman, W. C., J. R. Asbridge, S. J. Bame, and J. T. Gosling (1977), Plasma and magnetic fields from the Sun, in *The Solar Output and its Variation*, edited by O. R. White, pp. 351–382, Colo. Univ. Press, Boulder, Colo.

Fisk, L. A., T. H. Zurbuchen, and N. A. Schwadron (1999), On the coronal magnetic field: Consequences of large-scale motions, *Astrophys. J.*, *521*, 868–877.

Geiss, J., G. Gloeckler, and R. von Steiger (1995), Origin of the solar wind from composition data, *Space Sci. Rev.*, *72*, 49–60.

Gloeckler, G., et al. (1998), Investigation of the composition of solar and interstellar matter using solar wind and pickup ion measurements with SWICS and SWIMS on the ACE spacecraft, *Space Sci. Rev.*, *86*, 495.

Goldstein, M. L., and D. A. Roberts (1995), Magnetohydrodynamic turbulence in the solar wind, *Annu. Rev. Astron. Astrophs.*, *33*, 283–325.

Gosling, J. T., V. Pizzo, and S. J. Bame (1973), Anomalously low proton temperatures in the solar wind following interplanetary shock waves—Evidence for magnetic bottles?, *J. Geophys. Res.*, *78*, 2001.

Gosling, J. T., J. R. Asbridge, S. J. Bame, and W. C. Feldman (1978), Solar wind stream interfaces, *J. Geophys. Res.*, *83*, 1401–1412.

Gosling, J. T., J. Birn, and M. Hesse (1995), Three-dimensional magnetic reconnection and the magnetic topology of coronal mass ejection events, *Geophys. Res. Lett.*, *22*, 869–872.

Ko, Y. K., G. Gloeckler, C. M. S. Cohen, and A. B. Galvin (1999), Solar wind ionic charge states during the Ulysses pole-to-pole pass, *J. Geophys. Res.*, *104*, 17,005–17,019.

Lepri, S. T., T. H. Zurbuchen, L. A. Fisk, I. G. Richardson, H. V. Cane, and G. Gloeckler (2001), Iron charge distribution as an identifier of interplanetary coronal mass ejections, *J. Geophys. Res.*, *106*, 29,231–29,238.

Li, H., S. P. Gary, and O. Stawicki (2001), On the dissipation of magnetic fluctuations in the solar wind, *Geophys. Res. Lett.*, *28*, 1347–1350.

McComas, D. J., S. J. Bame, P. Barker, W. C. Feldman, J. L. Phillips, P. Riley, and J. W. Griffee (1998), Solar wind electron proton alpha monitor (SWEPAM) for the advanced composition explorer, *Space Sci. Rev.*, *86*, 563.

McComas, D. J., H. A. Elliot, and R. von Steiger (2002), Solar wind from high-latitude coronal holes at solar maximum, *Geophys. Res. Lett.*, *29*(9), 1314, doi:10.1029/2001GL013940.

Richardson, I. G., and H. V. Cane (1995), Regions of abnormally low proton temperature in the solar wind (1965–1991) and their association with ejecta, *J. Geophys. Res.*, *100*, 23,397–23,412.

Roberts, D. A., and M. L. Goldstein (1991), Turbulence and waves in the solar wind, *Rev. Geophys.*, *29*, suppl., 932–943.

Siscoe, G. L., and D. Intriligator (1993), Three views of two giant streams: Aligned observations at 1 AU, 4.6 AU, and 5.9 AU, *Geophys. Res. Lett.*, *20*, 2267–2270.

Siscoe, G. L., B. Goldstein, and A. J. Lazarus (1969), An east-west asymmetry in the solar wind velocity, *J. Geophys. Res.*, *74*, 1759–1762.

Stone, E. C., A. M. Frandsen, E. R. Mewaldt, E. R. Christian, D. Margolies, J. F. Ormes, and F. Snow (1998), The Advanced Composition Explorer, *Space Sci. Rev.*, *86*, 1.

von Steiger, R., N. A. Schwadron, L. A. Fisk, J. Geiss, G. Gloeckler, S. Hefti, B. Wilken, R. F. Wimmer-Schweingruber, and T. H. Zurbuchen (2000), Composition of quasi-stationary solar wind flows from Ulysses/Solar Wind Ion Composition Spectrometer, *J. Geophys. Res.*, *105*, 27,217–27,238.

Wimmer-Schweingruber, R. F., R. von Steiger, and R. Paerli (1997), Solar wind stream interfaces in corotating interaction regions: SWICS/Ulysses results, *J. Geophys. Res.*, *102*, 17,407–17,417.

Zurbuchen, T. H., S. Hefti, L. A. Fisk, G. Gloeckler, and N. A. Schwadron (2000), Magnetic structure of the slow solar wind: Constraints from composition data, *J. Geophys. Res.*, *105*, 18,327–18,336.

Zurbuchen, T. H., L. A. Fisk, G. Gloeckler, and R. von Steiger (2002), The solar wind composition throughout the solar cycle: A continuum of dynamic states, *Geophys. Res. Lett.*, *29*(9), 1352, doi:10.1029/2001GL013946.

N. U. Crooker and A. C. Pagel, Center for Space Physics, Boston University, Boston, MA 02215, USA. (crooker@bu.edu; pagel@bu.edu)

J. T. Gosling, Space and Atmospheric Sciences (NIS-1), Los Alamos National Laboratory, P. O. Box 1663, MS D466, Los Alamos, NM 87545, USA. (jgosling@lanl.gov)

T. H. Zurbuchen, Department of Atmospheric, Oceanic, and Space Science, University of Michigan, 2455 Hayward Street, Ann Arbor, MI 48109-2143, USA. (thomasz@umich.edu)